

Geochronology and Hf Isotope Study of Pegmatite in the Xiaoqinling Area of NW China: Implication for Petrogenesis and Regional Metamorphism

Haixiang Zhao¹, Shaoyong Jiang^{*2,3}, Baozhang Dai³, Liang Ma³, Jianwei Li²

1. School of Earth Sciences and Engineering, Hohai University, Nanjing 210098, China

2. State Key Laboratory of Geological Processes and Mineral Resources, Faculty of Earth Resources, China University of Geosciences, Wuhan 430074, China

3. State Key Laboratory for Mineral Deposits Research, School of Earth Sciences and Engineering, Nanjing University, Nanjing 210093, China

ABSTRACT: In this study, we carried out petrography, zircon U-Pb geochronology and Hf isotopic analyses on a granitic pegmatite dyke in the Xiaoqinling area in southern margin of the North China Craton (NCC). Our study suggests that the pegmatite dyke likely crystallized from a volatile-rich pegmatitic magma. Different from most other pegmatite elsewhere, zircon from this pegmatite dyke does not contain unusually high U and Th concentrations and suffered no evident radioactive damage, therefore we successfully obtained a zircon U-Pb dating using laser ablation-inductively coupled plasma-mass spectrometry (LA-ICP-MS), which yields an average $^{207}\text{Pb}/^{206}\text{Pb}$ age of $1\,814\pm 6$ Ma, representing the intrusive age of the granitic pegmatite dyke. Zircon $\varepsilon_{\text{Hf}}(t)$ values are between -8.3 and -3.0, corresponding to Hf depleted mantle model ages from 2 649 to 2 991 Ma with an average of 2 881 Ma. These data indicate that this granitic pegmatite dyke may have been derived from partial melting of Meso-Neoproterozoic metamorphic rocks from the Xiaoqinling basement. Granitic pegmatite magma may have emplaced within the Taihua Group wall rocks during the last stage of the middle to high grade metamorphism. Furthermore, according to the petrographic observation, the 1.81 Ga pegmatite dyke and the 1 800–1 750 Ma Xiong'er Group rocks were not undergone middle to high grade metamorphism, indicating 1.81 Ga as the termination of the latest regional metamorphism in the southern margin of the NCC.

KEY WORDS: Xiaoqinling, pegmatite, zircon U-Pb dating, Hf isotope, metamorphism.

0 INTRODUCTION

Age dating and petrogenesis of pegmatite are two long standing problems attracting attentions of many geologists. Ages of pegmatite have traditionally been determined by a variety of isotope dating methods such as K-Ar, Ar-Ar and Rb-Sr isochron methods (e.g., Singh and Chabria, 2002), which are all not reliable because these systems can be easily disturbed by later hydrothermal alteration and geological overprinting. In recent years, in-situ U-Pb dating of zircon by sensitive high-resolution ion microprobe (SHRIMP) and LA-ICP-MS has been widely used. However, zircons from most pegmatites may have unusually high U and Th contents that can potentially cause radioactive damage to the crystal lattice of zircon. In this case, later hydrothermal overprinting may lead to incongruent dissolution and re-crystallization of zircon and

consequently the disturbance of the U-Pb isotope systematics (Kusiak et al., 2009; Geisler et al., 2007, 2002; Söderlund, 1996). Therefore, these zircons are not suitable for precisely dating the age of pegmatite. For example, the formation age for one of the largest pegmatite in the world, the Altai No. 3 granitic pegmatite in Northwest China, is controversial because high U and Th contents leading to the crystal damage of zircon grains (Zhong et al., 2011; Wang et al., 2007).

Regarding the petrogenesis of granitic pegmatite, most people believed that pegmatite was formed by slow and sufficient fractional crystallization of volatile-rich magma under favorable conditions (London and Morgan, 2012; Jahns and Burnham, 1969). This independent high volatile pegmatite magma could be derived from the convergence of volatile components at the late stage of the magma crystallization, or from partial melting of rocks during metamorphism accompanied by migmatization. Alternatively some people suggested that pegmatite may be formed by late hydrothermal alteration of aplite or granite (e.g., Gresens, 1967), against the existence of independent pegmatitic magma. Hf isotope study of zircon from pegmatite can be used to determine the sources of pegmatitic magma and hence can help in understanding the petroge-

*Corresponding author: shyjiang@cug.edu.cn

© China University of Geosciences and Springer-Verlag Berlin Heidelberg 2015

Manuscript received December 10, 2014.

Manuscript accepted April 3, 2015.

nesis of pegmatite. In addition, the study of pegmatite can also provide valuable information on metamorphic history, kinematic stages of collisional belt, and rare metal mineralization (Gilotti et al., 2014; Santosh and Collins, 2003; Araújo et al., 2001; Tadesse, 2001; Semenov and Santosh, 1997).

The Xiaoqinling area is the second largest gold producing center in China and is located in a basement-cored uplift along the southern margin of the NCC. Numerous pegmatite dykes occur in the Xiaoqinling area. Previous studies indicated pegmatite dykes were dated at 143 ± 1 , $1\ 806\pm 3$ and $1\ 955\pm 30$ Ma (Deng et al., 2013; Li et al., 2007; Lu et al., 1997), indicating that they could be the products of several tectono-thermal events. Therefore, the exact formation time of these pegmatite dykes need to be further verified. Furthermore, the study of the pegmatites can also yield new information on the metamorphism history of the southern margin of the NCC, which is still controversial despite of lots of studies (Shi et al., 2011; Liu et al., 2009; Xu et al., 2009; Yang, 2008; Li et al., 2007; Wan et al., 2006; Ni et al., 2003).

In this paper we present petrography, zircon U-Pb dating and Hf isotopic studies of a granitic pegmatite dyke intruded into the Taihua Group basement rocks in the Xiaoqinling area in an attempt to determine the formation age, constrain the petrogenesis, and discuss implications for the tectono-thermal event and regional metamorphism in the area.

1 GEOLOGICAL SETTING

The Xiaoqinling area is located in a basement-cored uplift

at the southmost part of the Trans-North China orogen (TNCO), which is considered a continent-continent collision belt along which the eastern and western blocks amalgamated to form the coherent basement of the NCC (Wang et al., 2010; Zhao et al., 2008; Kusky et al., 2007; Wu et al., 2005). The nearly E-W-trending Taiyao fault and Xiaohe fault bound the district to the north and the south, respectively. The Xiaoqinling area contains amphibolite- to granulite-facies metamorphic rocks of the Taihua Group, mainly amphibolite, biotite-plagioclase gneiss, migmatite, quartzite, and marble (Fig. 1). The Taihua Group rocks also occurred in the other old terranes, i.e., Xiaoshan, Xiong'er shan, Lushan and Wuyang, which all scatter along the southern margin of the NCC. Previous researchers have reported various ages for the Taihua Group ranging from the Late Archean to the Paleoproterozoic using different methods such as paleontology, Rb-Sr, Sm-Nd, Ar-Ar, and zircon Pb-Pb dating (Ni et al., 2003; Zhou et al., 1998; Ding 1996; Xue et al., 1995; Kröner et al., 1988). Recently, the application of SHRIMP and LA-ICP-MS to in situ U-Pb zircon geochronology confirmed the Late Archean to Paleoproterozoic ages of the Taihua Group (Yu et al., 2013; Diwu et al., 2010, 2007; Liu et al., 2009; Xu et al., 2009; Yang, 2008; Li et al., 2007; Wan et al., 2006). Then these terranes underwent complex tectonic-thermal history and the Taihua Group rocks were metamorphosed to amphibolite- to granulite-facies. The voluminous Paleoproterozoic (1 800–1 750 Ma) volcanic rocks of the Xiong'er Group (Wang et al., 2010; Zhao et al., 2004), which formed on top of most of the southern NCC, are absent from the Xiaoqinling area.

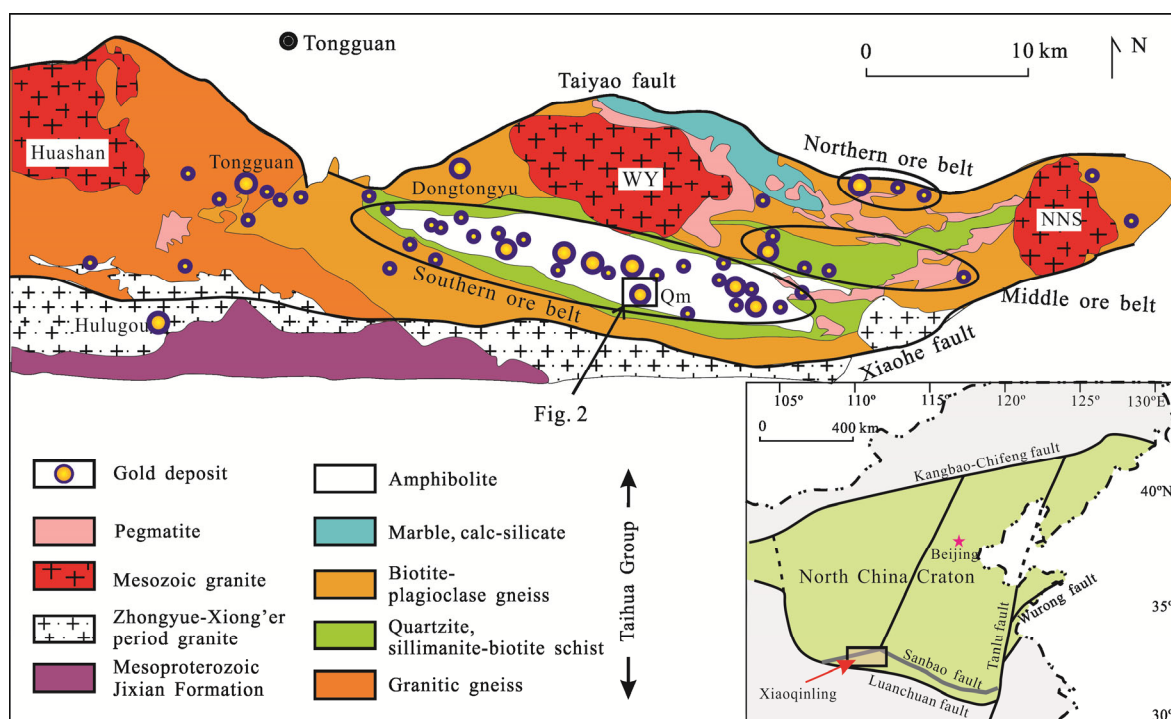


Figure 1. Simplified geological map of the Xiaoqinling area (modified after Jiang et al., 2009; Chen, 2006; Fan et al., 2000).

The main geologic structures of the Xiaoqinling area are approximately E-W-trending faults and folds. The folds are Precambrian, while the faults have been proposed to have evolved from Triassic south-directed thrusting to Cretaceous

north-directed normal faulting (Li et al., 2011; Zhang et al., 1998). The main regional faults in the area, the Taiyao, Huan-chiyu, Guanyintang, and Xiaohe faults, from north to south, are 20 to 75 km long. Second-order faults in the area also trend E-W

mainly. Within the Xiaoqinling area, many gold bearing quartz veins as well as various kinds of dykes mainly occur in the second-order E-W-trending brittle-ductile and brittle fault belts.

Multiple magmatic events are recognized in the area, from the Palaeoproterozoic Guijiayu biotite-hornblende granite and Xiaohe biotite granite to the Late Mesozoic Wenyu and Niangniangshan biotite monzogranites. The two Mesozoic plutons which intruded the western and eastern parts of the area at about 130 Ma (Zhao et al., 2012) are the largest and exposed over an area of about 65 and 33 km², respectively.

Different kinds of dykes, including pegmatite, dolerite, lamprophyre are widespread in the area. The ages of the dykes are poorly constrained. According to Luan et al. (1985), at least two generations of intermediate-basic dykes exist in this area: Caledonian gabbro-dolerite dykes with a K-Ar whole rock age of 418 Ma and Early Yanshanian dolerite dykes with a K-Ar whole rock age of 182–148 Ma. SHRIMP U-Pb dating of magmatic zircon by Wang et al. (2008) gave ages of 126.9±4.8 and 128.6±4.7 Ma which may date another stage of mafic dyke intrusion. However, Bi et al. (2011) reported a zircon LA-ICP-MS ²⁰⁷Pb/²⁰⁶Pb age of 1 819±10 Ma (1σ) by analyzing four mafic dyke samples in the Xiaoqinling area. Thus they suggested that numerous mafic dykes in the Xiaoqinling area should have formed in Palaeoproterozoic, in an extensional setting after the collision between the eastern and western blocks of the NCC at ca. 1.85 Ga, and they suggested that the previous whole rock K-Ar and Rb-Sr ages which are significantly younger should represent thermal perturbation caused by Mesozoic tectonic-thermal event.

Pegmatites in the Xiaoqinling area mostly occur as veins, dendritic or irregular stocks within the Taihua Group metamorphic basement or in the contact zone of Taihua Group rocks and Mesozoic granite. They usually have sharp boundaries with the wall rocks. They are gray, light pinkish or greenish color, with granitic pegmatitic texture and massive structure. Deng et al. (2013) divided the pegmatites in the Xiaoqinling area into two groups. Group one dykes strike 275°–300° and typically contain K-feldspar, quartz, and plagioclase. They usually emplaced during the 2.0–1.8 Ga interval, which are thought to be related to the migmatization and magmatism (Li et al., 2007).

Group two dykes mostly strike northeast and emplaced at about 143 Ma (Deng et al., 2013). They mainly consist of albite and quartz. The studied pegmatite dyke in this paper strikes nearly east-west and has some petrographic similarities with the Group one dykes.

2 PETROGRAPHY

The sample XQL-148 was taken from a pegmatite dyke in the Qiangma gold deposit (Fig. 2). In this medium-large gold deposit, thirteen gold-bearing quartz veins have been identified with ten of them trending E-W. Sample XQL-148 was collected near the No. 10 pit of the Qiangma gold deposit at 34°23'17.3"N, 110°31'19.3"E (1 498 m above sea-level). This dyke intruded in the Taihua Group and shows no obvious deformation.

The greenish-gray pegmatite (Fig. 3a) with granitic pegmatitic texture consists of plagioclase (40 vol.%), alkali feldspar (30 vol.%), quartz (25 vol.%) and magnetite (4 vol.%, Fig. 3b). Accessory minerals include allanite, monazite, rutile, epidote, zircon and apatite. Alteration products are white mica, chlorite, epidote and locally calcite.

Plagioclase (1.6–10 mm in size) occurs as anhedral grains and shows polysynthetic twins (albite and pericline laws). More anorthite-rich compositions, usually the cores, appear saussuritized. Relatively large white mica shows orientations preferably parallel to the cleavage planes of plagioclase (Fig. 3c). Plagioclase is separated from magnetite by white mica. Locally plagioclase was corroded (interrupted twin lamellae) and the space filled with anhedral magnetite, rutile and white mica (Fig. 3d). Alkali feldspar (2.4 to 7.2 mm in size) is perthitic microcline and far less altered than the plagioclase. Perthite formation led to the exsolution of hematite inside the lamellae. Quartz forms large anhedral grains (0.4 to 10 mm in size) and shows intensive subgrain formation, usually with wavy extinction. Subgrain formation was oriented with respect to stress direction of the brittle deformation. Magnetite grains range in size from 0.01 mm to several mm. Small magnetite grains are dispersed in the whole rock. Large magnetite grains are anhedral and they occur together with allanite, rutile and zircon (Fig. 3e). Oxidation of magnetite to hematite along rims and cracks is common (Fig. 3e). Anhedral rutile occurs as rims and as

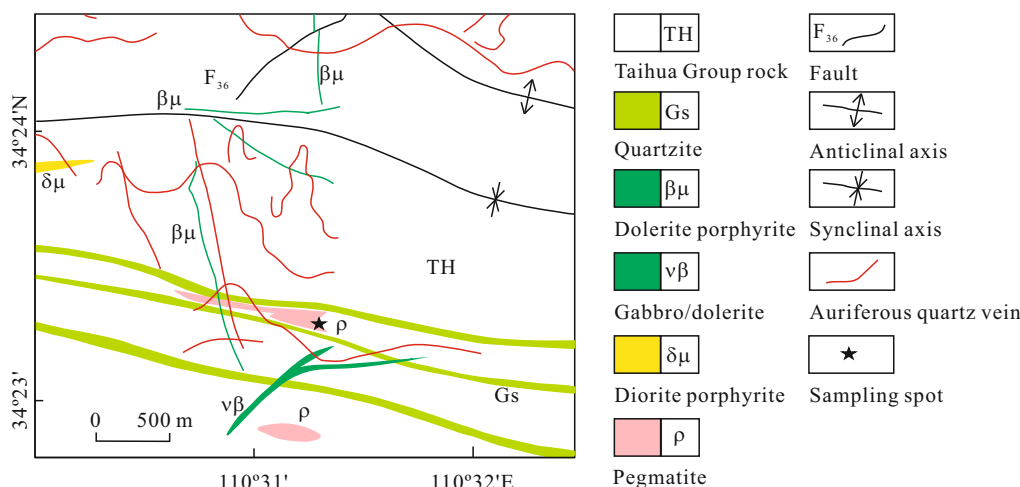


Figure 2. Simplified geological map of the Qiangma gold deposit in the Xiaoqinling area.

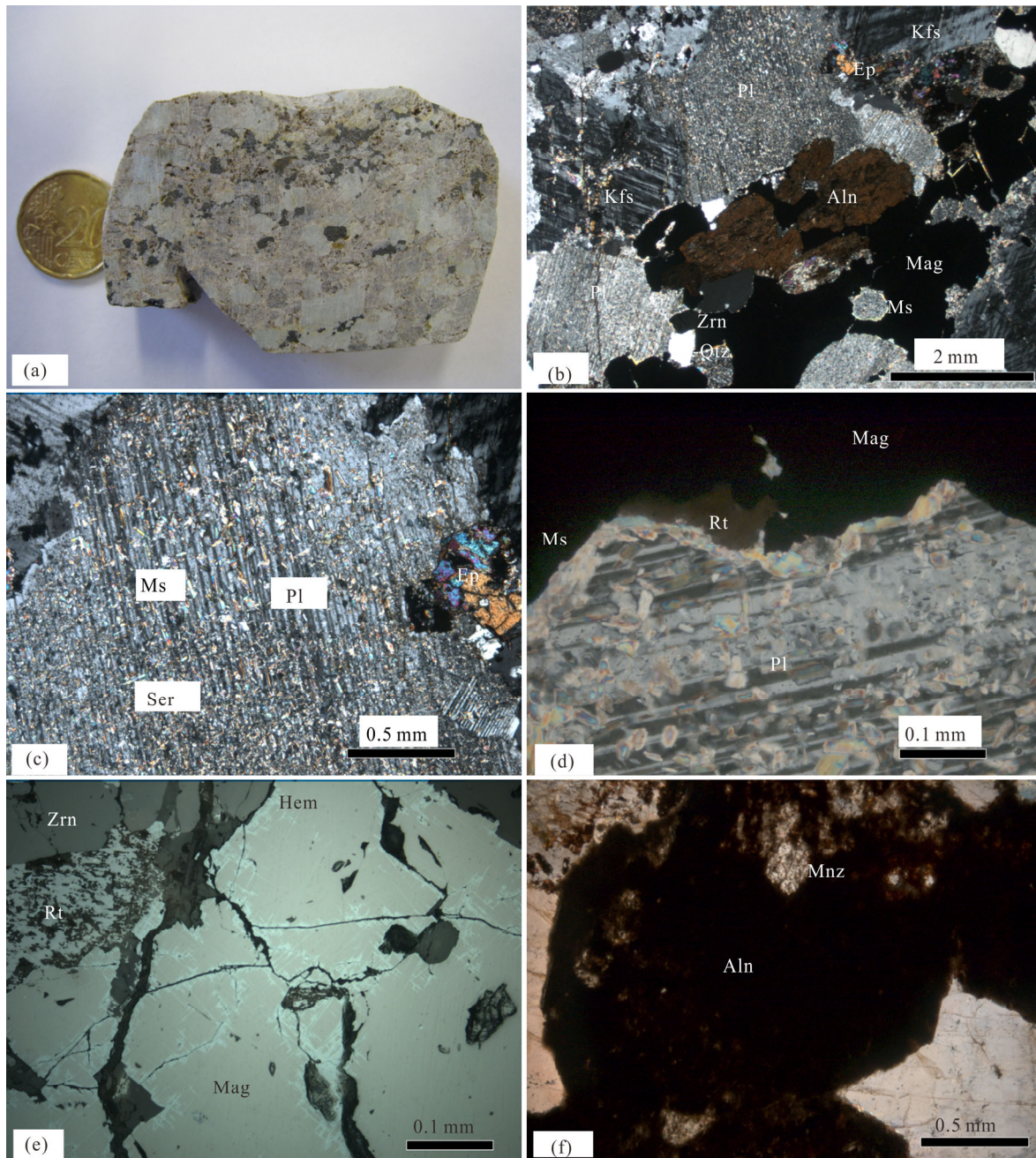


Figure 3. Photo of hand specimen (a) and photomicrography ((b)–(f), crossed polarizers) of the granitic pegmatite from the Xiaoqinling area. (a) Photo of sample XQL-148 showing greenish-gray granitic pegmatite with granitic pegmatitic texture. The diameter of the coin is 22.25 mm; (b) overview photomicrography of the granitic pegmatite showing plagioclase with polysynthetic twins altered to white mica and epidote, K feldspar with microcline twins, magnetite with white mica at the boundaries to plagioclase, brown allanite with brown-black decomposed core, and euhedral zircon; (c) plagioclase with polysynthetic twins and alteration to sericite, muscovite and epidote; (d) plagioclase was corroded (interrupted twin lamellae) and the space filled by anhedral magnetite, rutile and white mica; (e) large anhedral magnetite occurs together with rutile and zircon. Oxidation of magnetite to hematite occurs at the rims and along cracks; (f) monazite as anhedral inclusions in allanite. Pl. Plagioclase; Kfs. alkali feldspar; Qtz. quartz; Aln. allanite; Mag. magnetite; Zrn. zircon; Ms. muscovite; Ser. sericite; Ep. epidote; Rt. rutile; Hem. hematite; Mnz. monazite.

inclusions associated with cracks in magnetite.

Allanite grains, which reach up to 5 mm in size, appear heterogeneous. Small monazite and thorite grains occur as anhedral inclusions in allanite (Fig. 3f). Zircon occurs as edge-rounded subhedral grains (0.25 to 1.6 mm in size) with typically pale-pink colors and areas of different color intensity

are juxtaposed. The zircon grains show oscillatory magmatic zonation. Apatite occurs as anhedral to subhedral grains (0.08 to 0.6 mm in size) aligned along quartz boundaries. Both chlorite and epidote occur as alteration products in plagioclase. Chlorite forms subhedral laths (up to 0.1 mm long) and is partly altered to a yellow-brown phase. Epidote (0.06 to 0.3 mm in

size) occurs as subhedral colorless crystals. White mica resulted from the alteration of plagioclase is also present as sericite crack filling in magnetite and feldspars.

Later tectonic overprinting is indicated by systems of cracks (width 0.02 to 0.06 mm) filled by cataclastic feldspar and quartz as well as white mica. Goethite occurs along fractures and grain boundaries.

3 ANALYTICAL METHODS

The zircon grains for U-Pb dating were separated through crushing, conventional magnetic and heavy liquid separations, and then handpicked under a binocular microscope. The zircon grains were mounted in epoxy, and then polished to section the crystals in half for analysis. Zircon grains were documented with transmitted and reflected light micrographs as well as cathodoluminescence (CL) images, to reveal their internal structures. The CL images were obtained on an electron microprobe at the State Key Laboratory of Continental Dynamics, Northwest University, Xi'an. Zircon U-Pb dating was carried out on an Agilent 7500a ICP-MS equipped with a new wave research 213 nm laser ablation system at the State Key Laboratory for Mineral Deposits Research, Nanjing University. The ablated material was transported in a He carrier gas through 3 mm i.d. PVC tubing and then combined with Ar in a 30 cm³ mixing chamber prior to entering the ICP-MS for isotopic measurement. Mass discrimination of the mass spectrometer and residual elemental fractionation were corrected by calibration against a homogeneous zircon standard, GEMOC/GJ-1 (608 Ma). Samples are analyzed in 'runs' of ca. 15 analyses (10–12 unknowns, bracketed by 2–4 analyses of the standard). The 'unknowns' include one analysis of well-characterized zircon grains (mud tank, 735 Ma) that were analyzed frequently as an independent control on reproducibility and instrument stability. Analyses were carried out with a beam diameter of 30–40 μm, 5 Hz repetition rate, and energy of 10–20 J/cm². Data acquisition for each analysis took 100 s (40 s on background, 60 s on signal). Raw count rates for ²⁰⁶Pb, ²⁰⁷Pb, ²⁰⁸Pb, ²³²Th, and ²³⁸U were collected for age determination. Detailed analyt-

ical procedures are similar to those described by Jackson et al. (2004). The raw ICP-MS data were exported in ASCII format and processed using GLITTER (Van Achterbergh et al., 2001). Common Pb contents were evaluated using the method described by Andersen (2002). The age calculations and plotting of concordia diagrams were made using Isoplot (v. 3.23) (Ludwig, 2003). Zircon Hf isotopic analyses were carried out in situ using a new wave research UP213 laser-ablation system, attached to a Neptune multi-collector ICP-MS at Institute of Mineral Resources, Chinese Academy of Geological Sciences, Beijing. Instrumental conditions and data acquisition were comprehensively described by Wu et al. (2006) and Hou et al. (2007). A stationary spot was used for analysis, with a beam diameter of either 40 or 55 μm. Helium was used as the carrier gas to transport ablated material from the laser-ablation cell after which it was mixed with Ar prior to entering the ICP-MS torch. In order to correct the isobaric interferences of ¹⁷⁶Lu and ¹⁷⁶Yb on ¹⁷⁶Hf, ¹⁷⁶Lu/¹⁷⁵Lu ratio of 0.026 58 and ¹⁷⁶Yb/¹⁷³Yb ratio of 0.796 218 (Chu et al., 2002) were used. Zircon GJ1 was used as the reference standard, with a weighted mean ¹⁷⁶Hf/¹⁷⁷Hf ratio of 0.282 008±6 (2σ, n=34) during the routine analyses. This is indistinguishable from a weighted mean ¹⁷⁶Hf/¹⁷⁷Hf ratio of 0.282 013±19 (2σ) from in situ analysis reported by Elhlou et al. (2006). For the calculation of ε_{Hf}(t) and Hf model ages, the following parameters were used: (¹⁷⁶Hf/¹⁷⁷Hf)_{CHUR}=0.033 2, (¹⁷⁶Hf/¹⁷⁷Hf)_{CHUR,0}=0.282 772 (Blichert-Toft and Albarède, 1997); (¹⁷⁶Lu/¹⁷⁷Hf)_{DM}=0.038 4, (¹⁷⁶Hf/¹⁷⁷Hf)_{DM}=0.283 25 (Griffin et al., 2000); λ_{Lu}=1.867×10⁻¹¹ yr⁻¹ (Söderlund et al., 2004); (¹⁷⁶Lu/¹⁷⁷Hf)_{CC}=0.015 (Griffin et al., 2002).

4 RESULTS

4.1 Zircon U-Pb Dating

The CL images of zircons, U-Pb dating spots and Hf analytic spots were shown in Fig. 4. The U-Pb dating results are summarized in Table 1 and the U-Pb Concordia diagrams are shown in Fig. 5.

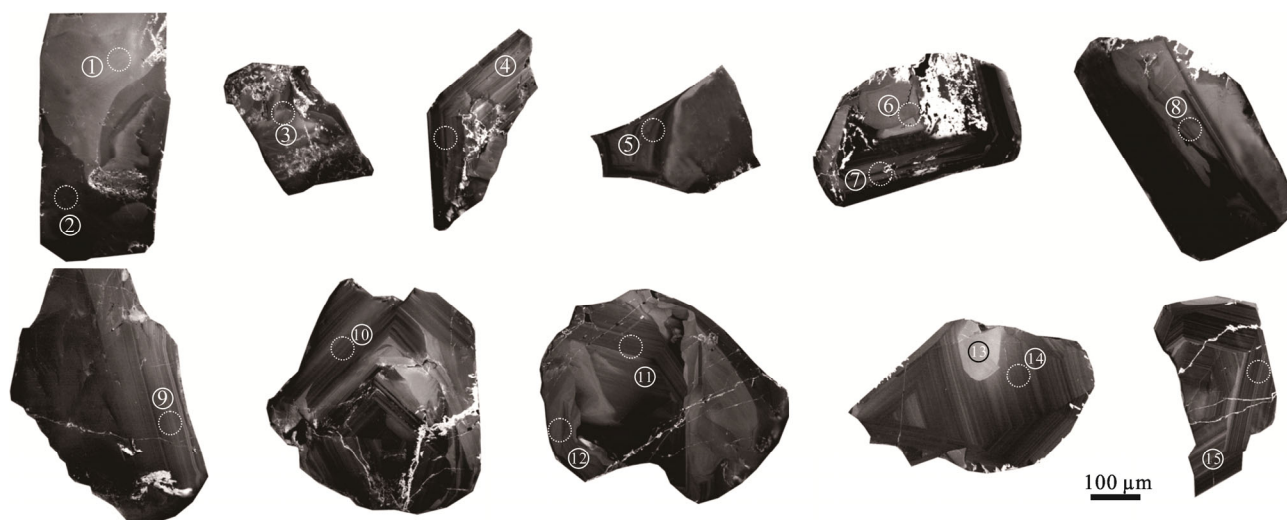


Figure 4. Zircon CL images of the granitic pegmatite from the Xiaoqinling area. Circles with numbers represent U-Pb dating spots and dotted line circles represent Hf analytic spots.

Table 1 U-Pb dating results of zircons from the granitic pegmatite in the Qiangma deposit, Xiaoqingling area

| Th (ppm) | U (ppm) | Th/U | $^{207}\text{Pb}/^{235}\text{U}$ | | $^{206}\text{Pb}/^{238}\text{U}$ | | $^{206}\text{Pb}/^{232}\text{Th}$ | | $^{207}\text{Pb}/^{206}\text{Pb}$ | | $^{207}\text{Pb}/^{235}\text{U}$ | | $^{206}\text{Pb}/^{238}\text{U}$ | | $^{208}\text{Pb}/^{232}\text{Th}$ | | | |
|-----------|---------|------|----------------------------------|------------|----------------------------------|------------|-----------------------------------|------------|-----------------------------------|------------|----------------------------------|------------|----------------------------------|------------|-----------------------------------|------------|-------|------------|
| | | | Ratio | 2 σ | Ratio | 2 σ | Ratio | 2 σ | Ratio | 2 σ | Ratio | 2 σ | Ratio | 2 σ | Ratio | 2 σ | Ratio | 2 σ |
| XQL148-01 | 11 | 199 | 0.05 | 0.0014 | 4.9472 | 0.0674 | 0.3232 | 0.0040 | 0.1113 | 0.0049 | 1.816 | 11 | 1.810 | 12 | 1.805 | 19 | 2.133 | 88 |
| XQL148-02 | 159 | 339 | 0.47 | 0.0014 | 5.0737 | 0.0699 | 0.3321 | 0.0041 | 0.0862 | 0.0039 | 1.813 | 11 | 1.832 | 12 | 1.849 | 20 | 1.672 | 72 |
| XQL148-03 | 171 | 308 | 0.55 | 0.0016 | 5.2626 | 0.0797 | 0.3421 | 0.0041 | 0.1049 | 0.0074 | 1.825 | 13 | 1.863 | 13 | 1.897 | 20 | 2.016 | 135 |
| XQL148-04 | 175 | 252 | 0.69 | 0.0014 | 5.1575 | 0.0739 | 0.3357 | 0.0042 | 0.0817 | 0.0038 | 1.823 | 12 | 1.846 | 12 | 1.866 | 20 | 1.586 | 70 |
| XQL148-05 | 188 | 243 | 0.77 | 0.0014 | 5.0508 | 0.0713 | 0.3324 | 0.0041 | 0.0814 | 0.0039 | 1.803 | 11 | 1.828 | 12 | 1.850 | 20 | 1.581 | 72 |
| XQL148-06 | 77 | 177 | 0.44 | 0.0015 | 4.9973 | 0.0726 | 0.3270 | 0.0040 | 0.0900 | 0.0050 | 1.814 | 12 | 1.819 | 12 | 1.824 | 20 | 1.741 | 93 |
| XQL148-07 | 207 | 322 | 0.65 | 0.0015 | 5.0379 | 0.0729 | 0.3287 | 0.0040 | 0.0867 | 0.0049 | 1.818 | 12 | 1.826 | 12 | 1.832 | 20 | 1.680 | 91 |
| XQL148-08 | 102 | 167 | 0.61 | 0.0013 | 4.9435 | 0.0745 | 0.3251 | 0.0040 | 0.0836 | 0.0049 | 1.804 | 12 | 1.810 | 13 | 1.814 | 20 | 1.623 | 92 |
| XQL148-09 | 542 | 633 | 0.86 | 0.0015 | 4.9495 | 0.0708 | 0.3227 | 0.0039 | 0.0834 | 0.0050 | 1.820 | 12 | 1.811 | 12 | 1.803 | 19 | 1.620 | 93 |
| XQL148-10 | 417 | 448 | 0.93 | 0.0015 | 4.9436 | 0.0717 | 0.3224 | 0.0039 | 0.0846 | 0.0054 | 1.820 | 12 | 1.810 | 12 | 1.801 | 19 | 1.641 | 100 |
| XQL148-11 | 278 | 371 | 0.75 | 0.0015 | 5.1555 | 0.0757 | 0.3375 | 0.0042 | 0.0868 | 0.0052 | 1.812 | 12 | 1.845 | 12 | 1.875 | 20 | 1.682 | 97 |
| XQL148-12 | 174 | 247 | 0.71 | 0.0015 | 4.9958 | 0.0745 | 0.3289 | 0.0041 | 0.0843 | 0.0054 | 1.802 | 12 | 1.819 | 13 | 1.833 | 20 | 1.636 | 100 |
| XQL148-13 | 108 | 190 | 0.56 | 0.0017 | 5.1098 | 0.0802 | 0.3321 | 0.0042 | 0.0863 | 0.0057 | 1.825 | 13 | 1.838 | 13 | 1.849 | 20 | 1.672 | 106 |
| XQL148-14 | 384 | 544 | 0.71 | 0.0016 | 4.9572 | 0.0785 | 0.3252 | 0.0041 | 0.0835 | 0.0061 | 1.809 | 13 | 1.812 | 13 | 1.815 | 20 | 1.622 | 113 |
| XQL148-15 | 223 | 371 | 0.60 | 0.0017 | 4.9660 | 0.0791 | 0.3268 | 0.0040 | 0.0923 | 0.0079 | 1.803 | 14 | 1.814 | 13 | 1.823 | 19 | 1.785 | 146 |

Most of the zircon grains in the pegmatite sample were broke due to their large size and during separation the rock was crushed too fine. However, in the CL images, most of the grains still show obvious oscillatory zoning, which is typical of magmatic zircon. Magmatic zircon grains usually have Th/U ratios greater than 0.1, while this ratio in metamorphic zircons is normally less than 0.1 (Belousova et al., 2002). In our analyses, Th and U concentrations are 11 ppm–542 ppm and 167 ppm–633 ppm, respectively. All of the Th/U ratios are between 0.44 and 0.93 (0.66 in average), except one analysis showing a Th/U ratio of 0.05 (Table 1).

The ²⁰⁷Pb/²⁰⁶Pb ages of all the analyzed spots (n=15) range

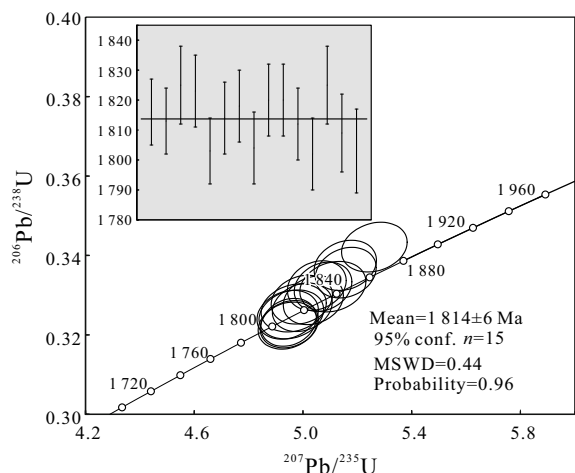


Figure 5. U-Pb Concordia plots of zircons in the granitic pegmatite from the Xiaoqingling area.

from 1 802 to 1 825 Ma. In the U-Pb concordia diagrams, all analyses form a tight cluster with a weighted mean ²⁰⁷Pb/²⁰⁶Pb age of 1 814±6 Ma (95% confidence, MSWD=0.44), which represents the age of the pegmatite.

4.2 Zircon Hf Isotopic Composition

The in situ Hf isotopic results of zircon are listed in Table 2 and shown in Fig. 6.

The results show that the initial ε_{Hf} (age corrected using U-Pb ages for individual grains) values for the pegmatite dyke are all negative, ranging from -8.3 to -3.0 (Table 2 and Fig. 6). Two-stage model ages (T_{DM}^C) were calculated (Table 2) by assuming a mean ¹⁷⁶Lu/¹⁷⁷Hf value of 0.015 for an average continental crust (Griffin et al., 2002), which gave T_{DM}^C ages of 2 649–2 991 Ma (2 881 Ma in average).

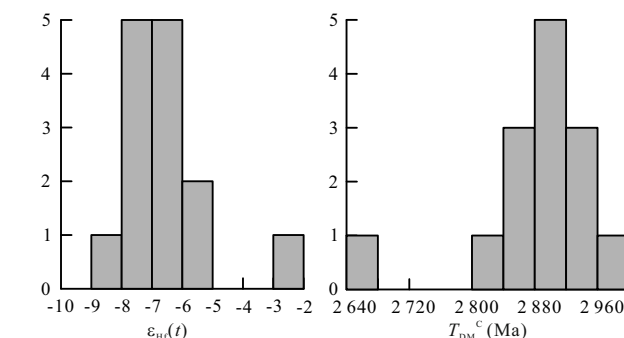


Figure 6. Histogram of ε_{Hf}(t) values and Hf model ages for zircons in the granitic pegmatite from the Xiaoqingling area.

Table 2 Hf isotope results of zircons from the granitic pegmatite in the Qiangma deposit, Xiaoqingling area

| | Age | ¹⁷⁶ Lu/ ¹⁷⁷ Hf | ¹⁷⁶ Hf/ ¹⁷⁷ Hf | | ε _{Hf} (0) | ε _{Hf} (t) | 2σ | T _{DM} | T _{DM} ^C | f _{Lu/Hf} |
|-----------|-------|--------------------------------------|--------------------------------------|-----------|---------------------|---------------------|-----|-----------------|------------------------------|--------------------|
| | (Ma) | ratio | Ratio | 2σ | | | | (Ma) | (Ma) | |
| XQL148-01 | 1 816 | 0.000 653 | 0.281 441 | 0.000 014 | -47.1 | -7.4 | 0.5 | 2 508 | 2 927 | -0.98 |
| XQL148-02 | 1 813 | 0.001 004 | 0.281 467 | 0.000 012 | -46.2 | -7.0 | 0.4 | 2 495 | 2 899 | -0.97 |
| XQL148-03 | 1 825 | 0.001 403 | 0.281 435 | 0.000 013 | -47.3 | -8.3 | 0.5 | 2 565 | 2 991 | -0.96 |
| XQL148-04 | 1 823 | 0.000 560 | 0.281 475 | 0.000 012 | -45.9 | -5.9 | 0.4 | 2 456 | 2 843 | -0.98 |
| XQL148-05 | 1 803 | 0.000 779 | 0.281 463 | 0.000 014 | -46.3 | -7.1 | 0.5 | 2 485 | 2 896 | -0.98 |
| XQL148-06 | 1 814 | 0.000 297 | 0.281 451 | 0.000 012 | -46.7 | -6.7 | 0.4 | 2 472 | 2 881 | -0.99 |
| XQL148-07 | 1 818 | 0.000 594 | 0.281 461 | 0.000 013 | -46.4 | -6.6 | 0.5 | 2 476 | 2 878 | -0.98 |
| XQL148-08 | 1 804 | 0.000 444 | 0.281 465 | 0.000 013 | -46.2 | -6.6 | 0.5 | 2 461 | 2 866 | -0.99 |
| XQL148-09 | 1 820 | 0.001 553 | 0.281 464 | 0.000 013 | -46.3 | -7.6 | 0.5 | 2 536 | 2 943 | -0.95 |
| XQL148-10 | 1 820 | 0.000 886 | 0.281 443 | 0.000 012 | -47.0 | -7.5 | 0.4 | 2 519 | 2 937 | -0.97 |
| XQL148-11 | 1 812 | 0.000 491 | 0.281 455 | 0.000 012 | -46.6 | -6.8 | 0.4 | 2 478 | 2 886 | -0.99 |
| XQL148-12 | 1 802 | 0.000 386 | 0.281 444 | 0.000 012 | -47.0 | -7.3 | 0.4 | 2 486 | 2 909 | -0.99 |
| XQL148-14 | 1 809 | 0.001 359 | 0.281 513 | 0.000 010 | -44.5 | -5.9 | 0.4 | 2 454 | 2 827 | -0.96 |
| XQL148-15 | 1 803 | 0.001 336 | 0.281 594 | 0.000 023 | -41.7 | -3.0 | 0.8 | 2 341 | 2 649 | -0.96 |

5 DISCUSSION

5.1 Crystallization Age of the Pegmatite Dyke

According to the field and microscopic observation, the granitic pegmatite dyke we studied was not undergone obvious metamorphism and deformation. In the CL images, the zircon grains show magmatic characteristics. Th and U concentrations are 11 ppm–542 ppm and 167 ppm–633 ppm, respectively, which are not extremely high as many other pegmatites. These

zircon grains did not undergo intensive radioactive damage and they are suitable for U-Pb dating. Therefore, the zircon U-Pb age (1 814±6 Ma) should represent the crystallization age of the pegmatite. Previous researchers have reported some age data for pegmatites in this area. Lu et al. (1997) obtained single zircon U-Pb age of 1 806±3 Ma from a pegmatite from the Jindongcha gold deposit. Li et al. (2007) reported a SHRIMP U-Pb zircon age of 1 955±30 Ma for a granitic pegmatite from

the Dahu gold deposit and they regarded 1 900–2 000 Ma as the second stage of metamorphism in the Xiaoqinling area. Deng et al. (2013) found another timing of pegmatitic magmatism of about 143 Ma by zircon and columbite (Mn) U-Pb geochronology. Our age result is basically consistent with the age dated by Lu et al. (1997), but different from the results of Li et al. (2007) and Deng et al. (2013). This is probably because in the Xiaoqinling area, there are several periods of pegmatite intrusive event and our result represents one of them.

5.2 Pegmatite Petrogenesis and Its Significance

Most people believed that pegmatite was formed by slow and sufficient fractional crystallization of high volatile magma under favorable conditions. There are two prevailed hypotheses, one is the fractional crystallization of a flux-bearing granitic melt, and another emphasizes the interactions of an aqueous fluid with granitic melt (London and Morgan, 2012). A recent model also invokes the formation of a flux-enriched boundary layer of silicate liquid in advance of a crystallization front, but origin of the pegmatite is far from solved (London and Morgan, 2012).

In the Xiaoqinling area, pegmatite dykes were strictly controlled by regional NE-trending structures and show clear intrusive boundary with wall rocks, which are against the metasomatic theory. Therefore, the pegmatite dykes may have crystallized from high volatile silicic magma. This independent high volatile silicic magma could be derived from the convergence of volatile components at the late stage of the granitic magma crystallization, or from partial melting of rocks during the last stage of regional metamorphism accompanied by migmatization. During the period of the pegmatite intrusion (1 814±6 Ma), there are no coexisting granite found in the area, and it can be excluded that the pegmatite dyke was formed at the late stage of the granitic magma differentiation. During Late Paleoproterozoic (~1.85 Ga), amalgamation of the western and eastern blocks of the North China Craton accompanied by metamorphic and magmatic events which are recorded in many lithologies in the central zone (Zhao et al., 2008; Wan et al., 2006). As the temperatures increased during the last stage of metamorphism, partial melting of deep-seated source rocks could occur and the parental melts for pegmatite dykes formed. Folds and faults well developed in the Xiaoqinling area and some folds formed during Precambrian. Axes of folds and hanging wall of the deep faults were both the decompression belt. So fluids such as water and magmatic volatiles tend to transport and aggregate in these areas. High water pressure can reduce the melting temperature of the source rocks. Therefore these structural positions were in favor of partial melting, producing high volatile magma and consequently lead to crystallization of the pegmatite dyke. Furthermore, zircon Lu-Hf isotopic analyses of the pegmatite dyke show negative $\varepsilon_{\text{Hf}}(t)$ values of -8.3 to -3.0, with Hf depleted mantle model ages between 2 649 and 2 991 Ma (2 881 Ma in average). These data demonstrated that the pegmatite dyke may have been derived from partial melting of the Meso-Neoproterozoic metamorphic rocks from the Xiaoqinling basement, without significant addition of mantle-derived magma.

Because of limitation of the dating methods and different

explanation for dating results, different views have been proposed on the metamorphic history of the Taihua Group distributed at the southern margin of the NCC. Wan et al. (2006) and Yang (2008) believed that the metamorphism occurred at 1.87–1.84 Ga in the Lushan area, but Liu et al. (2009) did not agree this idea and they regarded 2.79–2.77 and 2.67–2.65 Ga as the metamorphism ages of the Taihua Group in the Lushan area. Xu et al. (2009) preferred 2.1 Ga as the metamorphism age at the Xiong'er and Xiaoqinling areas and they found no evidence for a ~1.85 Ga metamorphic event in this area. Ni et al. (2003) believed 2.3–2.4 Ga as the metamorphic age of the Xiong'er area. Li et al. (2007) took 2 400–2 600 and 1 900–2 000 Ma as the two periods for metamorphism in the Xiaoqinling area. Shi et al. (2011) suggested that the Xiaoqinling area underwent an important thermal event at ~1.91 Ga, which had relationship with the global collision event during Columbia supercontinent. As we discussed above, the formation of the pegmatite dyke was related with last stage of regional metamorphism accompanied by migmatization. However, both the studied pegmatite dyke and the Xiong'er Group rocks which formed at 1.80–1.75 Ga (Wang et al., 2010; Zhao et al., 2004) did not suffer metamorphism higher than greenschist facies. These facts indicate that 1.81 Ga could represent the termination of regional metamorphism in the Xiaoqinling area, which is consistent with the situation in the central-north segment of the central zone reported by Wang et al. (2010).

6 CONCLUSION

Zircon U-Pb geochronology and Hf isotopic analyses on a granitic pegmatite dyke in the Xiaoqinling area were carried out in this study. Zircon U-Pb dating using LA-ICP-MS yielded an average $^{207}\text{Pb}/^{206}\text{Pb}$ age of 1 814±6 Ma, which represents the intrusive age of the granitic pegmatite. The zircon $\varepsilon_{\text{Hf}}(t)$ values are between -8.3 and -3.0 and two stage model ages range from 2 649 to 2 991 with 2 881 Ma in average, and these data indicate that the pegmatite may have been derived from partial melting of the Meso-Neoproterozoic metamorphic rocks from the Xiaoqinling basement. Combined with field occurrence, we proposed that the pegmatite dyke was formed during the last stage of regional metamorphism of basement. Furthermore, according to the petrography observation, the 1.81 Ga pegmatite and 1 800–1 750 Ma Xiong'er Group rocks were not undergone middle to high-grade metamorphism, which indicate that the 1.81 Ga as the termination of the latest regional metamorphism in the region.

ACKNOWLEDGMENTS

This research was financially supported by the National Key Basic Research Program of China (No. 2006CB403506), the National Natural Science Foundation of China (No. 41203011) and the Fundamental Research Funds for the Central Universities (No. 2013B03014). We especially thank Lingbao Bureau of Geology and Mineral Resources for support in the field survey.

REFERENCES CITED

Andersen, T., 2002. Correction of Common Lead in U-Pb Analyses that do not Report ^{204}Pb . *Chemical Geology*,

- 192(1–2): 59–79
- Araújo, M. N. C., Alves da Silva, F. C., Jardim de Sá, E. F., 2001. Pegmatite Emplacement in the Seridó Belt, Northeastern Brazil: Late Stage Kinematics of the Brasiliano Orogen. *Gondwana Research*, 4(1): 75–85
- Belousova, E. A., Griffin, W. L., Reilly, S. Y. O., et al., 2002. Igneous Zircon: Trace Element Composition as an Indicator of Source Rock Type. *Contributions to Mineralogy and Petrology*, 143(5): 602–622
- Bi, S. J., Li, J. W., Li, Z. K., 2011. Geological Significance and Geochronology of Paleoproterozoic Mafic Dykes of Xiaoqinling Gold District, Southern Margin of the North China Craton. *Earth Science—Journal of China University of Geoscience*, 36(1): 17–32 (in Chinese with English Abstract)
- Blichert-Toft, J., Albarède, F., 1997. The Lu-Hf Isotope Geochemistry of Chondrites and the Evolution of the Mantle-Crust System. *Earth and Planetary Science Letters*, 148(1–2): 243–258
- Chen, Y. J., 2006. Orogenic-Type Deposits and Their Metallogenic Model and Exploration Potential. *Chinese Geology*, 33(6): 1181–1196 (in Chinese with English Abstract)
- Chu, N. C., Taylor, R. N., Chavagnac, V., et al., 2002. Hf Isotope Ratio Analysis Using Multi-Collector Inductively Coupled Plasma Mass Spectrometry: An Evaluation of Isobaric Interference Corrections. *Journal of Analytical Atomic Spectrometry*, 17(12): 1567–1574
- Deng, X. D., Li, J. W., Zhao, X. F., et al., 2013. U-Pb Isotope and Trace Element Analysis of Columbite-(Mn) and Zircon by Laser Ablation ICP-MS: Implications for Geochronology of Pegmatite and Associated Ore Deposits. *Chemical Geology*, 344: 1–11
- Ding, L. F., 1996. New Recognition to Taihua Complex in Xiaoqinling Mountain, West of Henan Province. *Journal of Xi'an College of Geology*, 18(4): 1–8 (in Chinese with English Abstract)
- Diwu, C. R., Sun, Y., Lin, C. L., et al., 2007. Zircon U-Pb Ages and Hf Isotopes and Their Geological Significance of Yiyang TTG Gneisses from Henan Province, China. *Acta Petrologica Sinica*, 23(2): 253–262 (in Chinese with English Abstract)
- Diwu, C. R., Sun, Y., Lin, C. L., et al., 2010. LA-(MC)-ICP-MS U-Pb Zircon Geochronology and Lu-Hf Isotope Compositions of the Taihua Complex on the Southern Margin of the North China Craton. *Chinese Science Bulletin*, 55(23): 2557–2571
- Elhlou, S., Belousova, E., Griffin, W. L., et al., 2006. Trace Element and Isotopic Composition of GJ-Red Zircon Standard by Laser Ablation. *Geochimica et Cosmochimica Acta*, 70(18, Suppl. 1): A158
- Fan, H. R., Xie, Y. H., Zhao, R., et al., 2000. Dual Origins of Xiaoqinling Gold-Bearing Quartz Veins: Fluid Inclusion Evidence. *Chinese Science Bulletin*, 45(15): 1424–1430
- Geisler, T., Pidgeon, R. T., Kurtz, R., 2002. Transport of Uranium, Thorium, and Lead in Metamict Zircon Under Low-Temperature Hydrothermal Conditions. *Chemical Geology*, 191(1): 141–154
- Geisler, T., Schaltegger, U., Tomaschek, F., 2007. Re-Equilibration of Zircon in Aqueous Fluids and Melts. *Elements*, 3(1): 43–50
- Gilotti, J. A., McClelland, W. C., Wooden, J. L., 2014. Zircon Captures Exhumation of an Ultrahigh-Pressure Terrane, North-East Greenland Caledonides. *Gondwana Research*, 25(1): 235–256
- Gresens, R. L., 1967. Tectonic-Hydrothermal Pegmatites. I. The Model. *Contributions to Mineralogy and Petrology*, 15: 345–355
- Griffin, W. L., Pearson, N. J., Belousova, E., et al., 2000. The Hf Isotope Composition of Cratonic Mantle: LAM-MC-ICP-MS Analysis of Zircon Megacrysts in Kimberlites. *Geochimica et Cosmochimica Acta*, 64(1): 133–148
- Griffin, W. L., Wang, X., Jackson, S. E., et al., 2002. Zircon Chemistry and Magma Mixing, SE China: In-Situ Analysis of Hf Isotopes, Tonglu and Pingtan Igneous Complexes. *Lithos*, 61(3–4): 237–269
- Hou, K. J., Li, Y. H., Zou, T. R., et al., 2007. Laser Ablation-MC-ICP-MS Technique for Hf Isotope Microanalysis of Zircon and Its Geological Applications. *Acta Petrologica Sinica*, 23(10): 2595–2604 (in Chinese with English Abstract)
- Jackson, S. E., Pearson, N. J., Griffin, W. L., et al., 2004. The Application of Laser Ablation-Inductively Coupled Plasma-Mass Spectrometry to in Situ U-Pb Zircon Geochronology. *Chemical Geology*, 211(1–2): 47–69
- Jahns, R. H., Burnham, C. W., 1969. Experimental Studies of Pegmatite Genesis; I, A Model for the Derivation and Crystallization of Granitic Pegmatites. *Economic Geology*, 64(8): 843–864
- Jiang, S. Y., Dai, B. Z., Jiang, Y. H., 2009. Jiaodong and Xiaoqinling: Two Orogenic Gold Provinces Formed in Different Tectonic Settings. *Acta Petrologica Sinica*, 25(11): 2727–2738 (in Chinese with English Abstract)
- Kröner, A., Compston, W., Todt, W., et al., 1988. Age and Tectonic Setting of Late Archean Greenstone-Gneiss Terrain in Henan Province, China, as Revealed by Single-Grain Zircon Dating. *Geology*, 16(3): 211–215
- Kusiak, M. A., Dunkley, D. J., Slaby, E., et al., 2009. Sensitive High-Resolution Ion Microprobe Analysis of Zircon Re-equilibrated by Late Magmatic Fluids in a Hybridized Pluton. *Geology*, 37(12): 1063–1066
- Kusky, T., Li, J. H., Santosh, M., 2007. The Paleoproterozoic North Hebei Orogen: North China Craton's Collisional Suture with the Columbia Supercontinent. *Gondwana Research*, 12(1): 4–28
- Li, H. M., Chen, Y. C., Wang, D. H., et al., 2007. SHRIMP U-Pb Zircon Ages of Metamorphic Rocks and Veins in the Xiaoqinling Area, Henan, and Their Geological Significance. *Acta Petrologica Sinica*, 23(10): 2504–2512 (in Chinese with English Abstract)
- Li, N., Chen, Y. J., Fletcher, I. R., et al., 2011. Triassic Mineralization with Cretaceous Overprint in the Dahu Au-Mo Deposit, Xiaoqinling Gold Province: Constraints from SHRIMP Monazite U-Th-Pb Geochronology. *Gondwana Research*, 20: 543–552
- Liu, D. Y., Wilde, S. A., Wan, Y. S., et al., 2009. Combined

- U-Pb, Hafnium and Oxygen Isotope Analysis of Zircons from Meta-Igneous Rocks in the Southern North China Craton Reveal Multiple Events in the Late Mesoarchean–Early Neoproterozoic. *Chemical Geology*, 261(1–2): 140–154
- London, D., Morgan V. I. G. B., 2012. The Pegmatite Puzzle. *Element*, 8(4): 263–268
- Lu, S. N., Li, H. K., Li, H. M., et al., 1997. The Study on the Characteristics of Basement and Mineralization in Gold Concentrated Area—Take Xiaoqinling, Northern Hebei and Eastern Shandong Gold Districts as Examples. Geological Publishing House, Beijing. 113 (in Chinese)
- Luan, S. W., Cao, D. C., Fang, Y. K., et al., 1985. Geochemistry of Xiaoqinling Gold Deposits. *Journal of Mineralogy and Petrology*, 5(2): 1–118 (in Chinese with English Abstract)
- Ludwig, K. R., 2003. ISOPLOT 3.00: A Geochronology Toolkit for Microsoft Excel. Berkeley Geochronological Center Special Publication, Berkeley. 70
- Ni, Z. Y., Wang, R. M., Tong, Y., et al., 2003. $^{207}\text{Pb}/^{206}\text{Pb}$ Age of Zircon and $^{40}\text{Ar}/^{39}\text{Ar}$ of Amphibole from Plagioclase Amphibolite in the Taihua Group, Luoning, Henan, China. *Geological Review*, 49(4): 361–366 (in Chinese with English Abstract)
- Semenov, E., Santosh, M., 1997. Rare Metal Mineralization in Alkaline Pegmatites of Southern Indian Granulite Terrain. *Gondwana Research*, 1(1): 152–153
- Santosh, M., Collins, A. S., 2003. Gemstone Mineralization in the Palghat-Cauvery Shear Zone System (Karur-Kangayam Belt), Southern India. *Gondwana Research*, 6(4): 911–918
- Shi, Y., Yu, J. H., Xu, X. S., 2011. U-Pb Ages and Hf Isotope Compositions of Zircons of Taihua Group in Xiaoqinling Area, Shaanxi Province. *Acta Petrologica Sinica*, 27(10): 3095–3108 (in Chinese with English Abstract)
- Singh, Y., Chabria, T., 2002. Early Proterozoic ^{87}Rb - ^{86}Sr Model Ages of Pegmatitic Muscovite from Rare Metal-Bearing Granite-Pegmatite System of Kawadgaon, Bastar Craton, Central India. *Gondwana Research*, 5(4): 889–893
- Söderlund, U., 1996. Conventional U-Pb Dating Versus Single-Grain Pb Evaporation Dating of Complex Zircons from a Pegmatite in the High-Grade Gneisses of Southwestern Sweden. *Lithos*, 38(1–2): 93–105
- Söderlund, U., Patchett, P. J., Vervoort, J. D., et al., 2004. The ^{176}Lu Decay Constant Determined by Lu-Hf and U-Pb Isotope Systematics of Precambrian Mafic Intrusions. *Earth and Planetary Science Letters*, 219(3–4): 311–324
- Tadesse, S., 2001. Geochemistry of the Pegmatitic Rocks and Minerals in the Kenticha Belt, Southern Ethiopia: Implication to Geological Setting. *Gondwana Research*, 4(1): 97–104
- Van Acherbergh, E., Ryan, C. G., Jackson, S. E., et al., 2001. Data Reduction Software for LA-ICP-MS. In: Sylvester, P., ed., Laser-Ablation-ICP-MS in the Earth Sciences: Principles and Applications. Mineralogical Association of Canada, Ottawa. 239–243
- Wan, Y. S., Wilde, S. A., Liu, D. Y., et al., 2006. Further Evidence for ~1.85 Ga Metamorphism in the Central Zone of the North China Craton: SHRIMP U-Pb Dating of Zircon from Metamorphic Rocks in the Lushan Area, Henan Province. *Gondwana Research*, 9(1–2): 189–197
- Wang, J., Wu, Y. B., Gao, S., et al., 2010. Zircon U-Pb and Trace Element Data from Rocks of the Huai'an Complex: New Insights into the Late Paleoproterozoic Collision between the Eastern and Western Blocks of the North China Craton. *Precambrian Research*, 178(1): 59–71
- Wang, T. H., Mao, J. W., Wang, Y. B., 2008. Research on SHRIMP U-Pb Chronology in Xiaoqinling-Xiong'er Area: The Evidence of Delamination of Lithosphere in Qinling Orogenic Belt. *Acta Petrologica Sinica*, 24(6): 1273–1287 (in Chinese with English Abstract)
- Wang, T., Tong, Y., Jahn, B. M., et al., 2007. SHRIMP U-Pb Zircon Geochronology of the Altai No. 3 Pegmatite, NW China, and its Implications for the Origin and Tectonic Setting of the Pegmatite. *Ore Geology Reviews*, 32(1): 325–336
- Wang, X. L., Jiang, S. Y., Dai, B. Z., 2010. Melting of Enriched Archean Subcontinental Lithospheric Mantle: Evidence from the ca. 1 760 Ma Volcanic Rocks of the Xiong'er Group, Southern Margin of the North China Craton. *Precambrian Research*, 182(3): 204–216
- Wu, F. Y., Yang, Y. H., Xie, L. W., et al., 2006. Hf Isotopic Compositions of the Standard Zircons and Baddeleyites Used in U-Pb Geochronology. *Chemical Geology*, 234(1–2): 105–126
- Wu, F. Y., Zhao, G. C., Wilde, S. A., et al., 2005. Nd Isotopic Constraints on Crustal Formation in the North China Craton. *Journal of Asian Earth Sciences*, 24(5): 523–545
- Xu, X. S., Griffin, W. L., Ma, X., et al., 2009. The Taihua Group on the Southern Margin of the North China Craton: Further Insights from U-Pb Ages and Hf Isotope Compositions of Zircons. *Mineralogy and Petrology*, 97(1): 43–59
- Xue, L. W., Yuan, Z. L., Zhang, Y. S., et al., 1995. The Sm-Nd Isotope Age of Taihua Group in Lushan Area and Their Implications. *Geochimica*, 24(Suppl.): 92–97 (in Chinese with English Abstract)
- Yang, C. X., 2008. Zircon SHRIMP U-Pb Ages, Geochemical Characteristics and Environmental Evolution of the Early Precambrian Metamorphic Series in the Lushan Area, He'nan, China. *Geological Bulletin of China*, 27(4): 517–533 (in Chinese with English Abstract)
- Yu, X. Q., Liu, J. L., Li, C. L., et al., 2013. Zircon U-Pb Dating and Hf Isotope Analysis on the Taihua Complex: Constraints on the Formation and Evolution of the Trans-North China Orogen. *Precambrian Research*, 230: 31–44
- Zhang, J. J., Zheng, Y. D., Liu, S. W., 1998. The Xiaoqinling Metamorphic Core Complex: Structure, Genetic Mechanism and Evolution. China Ocean Press, Beijing. 120 (in Chinese)
- Zhao, G. C., Wilde, S. A., Sun, M., et al., 2008. SHRIMP U-Pb Zircon Ages of Granitoid Rocks in the Lüliang Complex: Implications for the Accretion and Evolution of the Trans-North China Orogen. *Precambrian Research*, 160(3): 213–226
- Zhao, H. X., Jiang, S. Y., Frimmel, H. E., et al., 2012. Geochemistry, Geochronology and Sr-Nd-Hf Isotopes of Two

- Mesozoic Granitoids in the Xiaoqinling Gold District: Implication for Large-Scale Lithospheric Thinning in the North China Craton. *Chemical Geology*, 294–295: 173–189
- Zhao, T. P., Zhai, M. G., Xia, B., et al., 2004. Zircon U-Pb SHRIMP Dating for the Volcanic Rocks of the Xiong'er Group: Constraints on the Initial Formation Age of the Cover of the North China Craton. *Chinese Science Bulletin*, 49(22): 2342–2349
- Zhong, L., Wang, Z. H., Liu, Y. L., 2011. The Geochronology Research Status of Altai Pegmatite, NW China: The Confusion of the Conventional Dating Methods Used in Granitic Magma. *Geochimica*, 29(4): 412–415 (in Chinese with English Abstract)
- Zhou, H. W., Zhong, Z. Q., Ling, W. L., et al., 1998. Sm-Nd Isochron for the Amphibolites within Taihua Complex from Xiaoqinling Area, Western Henan and its Geological Implications. *Geochimica*, 27(4): 367–372 (in Chinese with English Abstract)